Developmental Cell, Vol. 3, 367–381, September, 2002, Copyright ©2002 by Cell Press

Actin Cable Dynamics and Rho/Rock Orchestrate a Polarized Cytoskeletal Architecture in the Early Steps of Assembling a Stratified Epithelium

Alec Vaezi, Christoph Bauer, Valeri Vasioukhin,[2] and Elaine Fuchs[1]
Howard Hughes Medical Institute
Laboratory of Mammalian Cell Biology and Development
The Rockefeller University
New York, New York 10021

Summary

To enable stratification and barrier function, the epidermis must permit self-renewal while maintaining adhesive connections. By generating K14-GFP-actin mice to monitor actin dynamics in cultured primary keratinocytes, we uncovered a role for the actin cytoskeleton in establishing cellular organization. During epidermal sheet formation, a polarized network of nascent intercellular junctions and radial actin cables assemble in the apical plane of the monolayer. These actin fibers anchor to a central actin-myosin network, creating a tension-based plane of cytoskeleton across the apical surface of the sheet. Movement of the sheet surface relative to its base expands the zone of intercellular overlap, catalyzing new sites for nascent intercellular junctions. This polarized cytoskeleton is dependent upon α-catenin, Rho, and Rock, and its regulation may be important for wound healing and/or stratification, where coordinated tissue movements are involved.

Introduction

Cellular movements are important for organizing cells into three-dimensional tissues. Self-renewing, stratified tissues, such as skin epidermis, pose a particularly intriguing challenge in cellular dynamics. As dividing cells within the innermost basal layer of the epidermis detach from the underlying basement membrane of extracellular matrix (ECM), they withdraw from the cell cycle and move outward toward the skin surface. Basal keratinocytes draw together and fill vacancies created by departing cells, while differentiating suprabasal keratinocytes remain cohesive as they proceed on their upward trek. To perform its function as a barrier during development and wound healing, keratinocyte movement is enhanced, and this process is exaggerated.

The process of epidermal stratification begins with a monolayer of basal cells that assemble into a polarized sheet. The spatial cues that lead to their initial polarization are likely to be cell-ECM and cell-cell contacts (reviewed by Yeaman et al., 1999). Cell-ECM contacts are mainly mediated by transmembrane receptors of the integrin superfamily, whereas cell-cell contacts are mediated by homotypic interactions of the transmembrane family of cadherins. Biochemical and gene-targeting studies indicate that both types of junctions participate in establishing a polarized epidermal architecture (Hodivala and Watt, 1994; reviewed by Jamora and Fuchs, 2002).

Equally important, but less well understood, is the role of the actin cytoskeleton in generating the mechanical forces necessary to coordinate and stabilize adhesive structures and modulate changes in epithelial cell shape and motility. While αβ1 integrin's association with the actin cytoskeleton has been implicated in cellular migration, E-cadherin's link to the actin cytoskeleton is essential for strong cell-cell adhesion (Angres et al., 1996; Adams et al., 1998; Vasioukhin et al., 2000). These links are dynamic, and junction formation is accompanied by rearrangements in the actin cytoskeleton. When ECM triggers the clustering of αβ1 integrins into "focal contacts," a protein complex that includes vinculin and VASP converges concomitantly with the appearance of actin cables (stress fibers) at these sites (Reinhard et al., 1992). Recently it was shown that, during the early stages of intercellular adhesion, E-cadherin, β-catenin, and α-catenin assemble into clusters, or "puncta" (Yonemura et al., 1995; Adams et al., 1996), which also become the scene for localizing vinculin and VASP and reorganizing and polymerizing actin (Vasioukhin et al., 2000). Associating with each E-cadherin punctum is a radially arranged bundle of actin filaments, perpendicularly aligned with respect to the plasma membrane (Yonemura et al., 1995; Adams et al., 1996; 1998). In fully formed epithelial sheets, a cortical belt of actin cables underlies the intercellular junctures (Hirano et al., 1987).

The Rho family of small GTPases are candidates for at least partial regulation of these actin rearrangements. This family promotes the formation of integrin-mediated focal adhesions, stress fibers (Rho), lamellipodia (Rac), and filopodia (Cdc42) (Ridley and Hall, 1992; reviewed by Hall, 1998; Ridley, 2001). Rac has also been implicated in various intercellular processes, including adherens junction assembly (Braga et al., 1997; Takaishi et al., 1997; Jou and Nelson, 1998; Jou et al., 1998), and active Rac levels increase during the transition from isolated cells to a confluent epithelial sheet (Noren et al., 2001; Nakagawa et al., 2001). This said, all three subfamilies of Rho GTPases participate in intercellular junction formation in cultured epithelial cells and dorsal closure of epithelial sheets in vivo (Jacinto et al., 2002; Nakagawa et al., 2001, and the references therein). A major challenge still unsettled is the specific role that each of the GTPases plays in these epithelial actin dynamics.

To probe more deeply into the dynamics and regulation of the actin cytoskeleton during epithelial sheet formation and stratification, we engineered physiologically normal transgenic mice expressing GFP-actin in their skin keratinocytes. When cultured, these cells exhibited dramatic actin dynamics and cytoskeletal polarization as they organized into epidermal sheets and stratified tissue structures. During the initial process of

[1]Correspondence: fuchs@rockefeller.edu
[2]Present address: Division of Human Biology, Fred Hutchinson Cancer Research Center, 1100 Fairview Ave North C3-168, Seattle, Washington 98109.

sheet formation, a network of actin cables and adherens junction puncta assembled within the apical zone of the monolayer. This intermediate, encompassing actin bundles and nascent junctions, connected to myosin II-decorated actin cables, formed a cytoskeletal plane that spanned across the entire epidermal sheet. The apical network was dependent upon functional Rho and Rock and bore a marked resemblance to actin stress fibers and focal contacts at the base of the epithelium. This transient tension-based architecture of polarized cytoskeleton and adherens junctions may enable cells to physically draw over one another, generating new sites for cell-cell contacts in the process. Such a mechanism could be important for wound healing as well as for the formation of multilayered tissue structures.

Results

Generation of GFP-Actin Transgenic Mice

GFP-actin fusion protein has been widely employed to monitor actin in living cells (e.g., Doyle and Botstein, 1996; reviewed by Jacinto et al., 2002). We generated transgenic mice expressing EGFP-tagged murine β-actin under the control of the keratin 14 promoter/enhancer, functional in mitotically active epidermal cells (Figure 1A). Mice expressing the transgene were identified by the green fluorescent glow of the skin surface (Figures 1B and 1B′). To date, the seven founders and offspring of two propagated lines appear healthy and viable.

Analyses of frozen skin sections revealed keratinocyte-specific fluorescence throughout the cytoplasm and cell-cell borders (Figures 1C and 1D). Primary keratinocytes of the skins of newborn animals were then cultured, and protein extracts were prepared and used for SDS-PAGE and immunoblot analyses. An antibody against nonskeletal muscle actins detected two bands corresponding to the expected sizes of full-length GFP-actin (70 kDa) and endogenous actin (40 kDa) (Figure 1E). The identity of the GFP-actin band was confirmed with anti-GFP antibodies. By comparing the intensity of the GFP-actin band with that of different dilutions of endogenous actin, we estimated that GFP-actin accounted for ~2%–3% of the total actin for mouse line 50 (shown). Employing procedures to fractionate polymerized and monomeric actin (Cano et al., 1992), we found that GFP-actin and endogenous actin distributed similarly (25% ± 5%, polymerized; 75% ± 5%, monomeric) (Figure 1E). By these criteria, GFP-actin assembled efficiently into endogenous actin filaments in skin epidermal cells. Additional evidence in support of this point is provided below.

Actin Dynamics in Solitary Keratinocytes: Changes in the Actin Cytoskeleton that Are Not Dependent upon Adherens Junction Formation

We first explored actin dynamics in primary epidermal keratinocytes cultured under conditions where the cells are not already organized into tightly packed colonies. In low calcium medium, keratinocytes formed a robust network of fluorescing actin stress fibers, which also bound rhodamine-labeled phalloidin, a marker of polymerized actin (Figure 2A). The haze of GFP-actin surrounding the nucleus did not bind phalloidin but did colabel with anti-β-actin antibodies, reflective of an unpolymerized actin pool (data not shown). Overall, the patterns of transgenic and endogenous actin were indistinguishable.

In low calcium medium, GFP-actin-expressing primary keratinocytes extended numerous filopodia, lamellipodia, and ruffles, in a nonpolarized fashion (see Supplemental Movie S1 at http://www.developmentalcell.com/cgi/content/full/3/3/367/DC1; Figure 2). These extensions were as robust (if not more robust) when cultures were switched to high-calcium medium (see Supplemental Movie S1). Fluorescing actin filaments concentrated at the leading edges of these membrane ruffles, while a continuous flux of concentric rings of actin filaments moved centripetally from the cytoplasmic periphery toward the nucleus, where they subsequently disappeared (see Supplemental Movie S1).

When visual information is captured by video microscopy and presented as a kymograph, actin fiber movements can be monitored spatially over time. In analyzing the slopes of lines drawn through a filmed GFP-actin keratinocyte, we saw that the movements of actin fibers at ruffling edges were considerably faster than those of concentric actin rings (Figure 2B). The movement of actin rings seemed analogous to the rearward flow of actin filaments, "treadmilling," described previously and attributed to myosin pulling actin filaments toward the center of cells (for reviews, see Theriot, 1997; Carlier, 1998). Consistent with this notion, myosin II localized to these rings (see below).

Actin Dynamics during Epithelial Sheet Formation: Changes in the Actin Cytoskeleton that Are Dependent upon Calcium-Induced Adherens Junction Formation

Within several hours of switching the calcium concentration from 0.05 mM to 1.2 mM, keratinocytes form an intermediate structure, the adhesion zipper, on their way to assembling an epithelial sheet (Vasioukhin et al., 2000). Generated between neighboring epidermal cells, this structure is an active site of actin polymerization and consists of rows of E-cadherin, β-catenin, α-catenin, VASP, and vinculin complexes, each with an associated radial bundle of actin fibers (Vasioukhin et al., 2000; see also Yonemura et al. 1995; Adams et al., 1998). When K14-GFP-actin keratinocytes were subjected to calcium-induced intercellular adhesion, they formed adhesion zippers and epidermal sheets with similar kinetics to nontransgenic littermate keratinocytes (Figure 2C).

Video microscopy on living cells provided new insights into the process of adhesion zipper and epithelial sheet formation (see Supplemental Movie S2A at http://www.developmentalcell.com/cgi/content/full/3/3/367/DC1). During the first hour after the calcium switch, GFP-actin keratinocytes made numerous, but transient, contacts with their neighbors, often exhibiting extensive, but nonproductive, overlapping of adjacent membranes. On occasion, an intercellular contact resulted in a point of stable adhesion (Figure 3A). When this happened, the mechanical forces of retraction in the presence of a stable intercellular contact resulted in elongated finger-like projections, resembling those seen in fixed image microscopy (Figure 3B; Yonemura et al.,

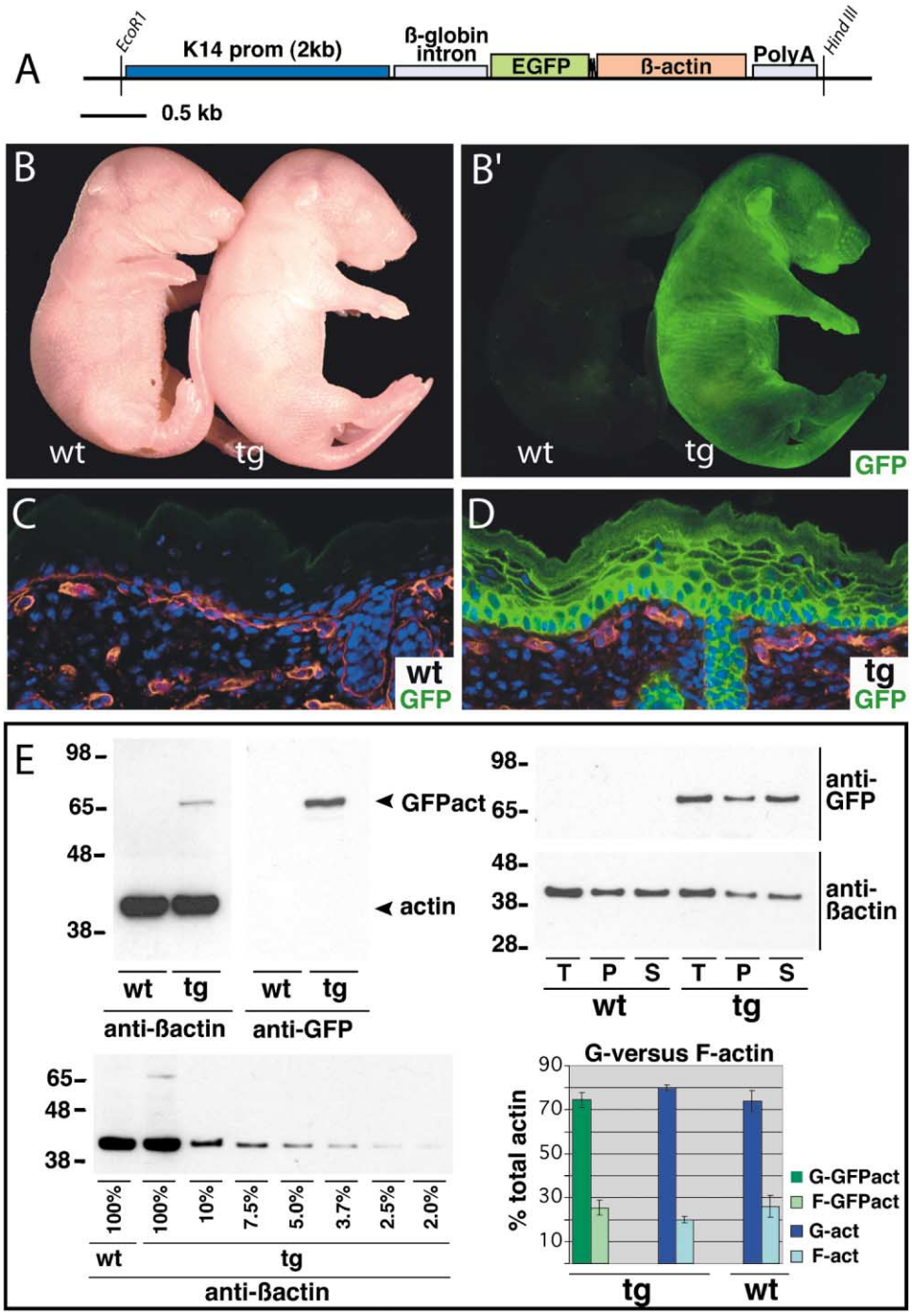

Figure 1. Expression and Quantitation of Levels of EGFP-Murine β-Actin Fusion Protein in Epidermal Keratinocytes of Transgenic Mice

(A) The K14-GFP-actin transgene construct, containing 2.1 kb of the human K14 promoter, rabbit β-globin intron, EGFP-actin cDNA (BD Biosciences, Palo Alto, CA), and K14 3′ untranslated and polyadenylation sequences.

(B–D) Littermate (wt) and transgenic (tg) mice and derived frozen skin sections visualized by epiluminescence and epifluorescence (GFP) microscopy. Anti-laminin, red; Dapi, blue.

(E) Quantitation of transgene expression. (Left panel, top) Immunoblot analyses of total protein extracts. Anti-β-actin panel antibody recognizes both GFP-actin and endogenous β-actin; anti-GFP antibody is transgene specific. Molecular mass markers at left are in kilodaltons. (Left panel, bottom) Anti-actin immunoblot analyses of total protein extracts. Serial dilutions of wild-type extracts were made in order to match the dilution (~2%–3%) where the wt actin band matched the intensity of the GFP-actin band, as judged by densitometry scanning of the blot. (Right panels) Cultured primary keratinocytes were lysed and processed for monomeric (G) versus filamentous (F) actin fractionation (see Experimental Procedures). Anti-GFP and anti-β-actin immunoblot analyses of equal amounts of total protein (T), pellet (P; F-actin) and supernatant (S; G-actin) fractions. The blot was then subjected to densitometry scanning. The graph below depicts the percentages of G- and F-actin in the samples. Note that these values were similar for keratinocytes cultured in either low (0.05 mM; shown)- or high (1.2 mM)-calcium medium.

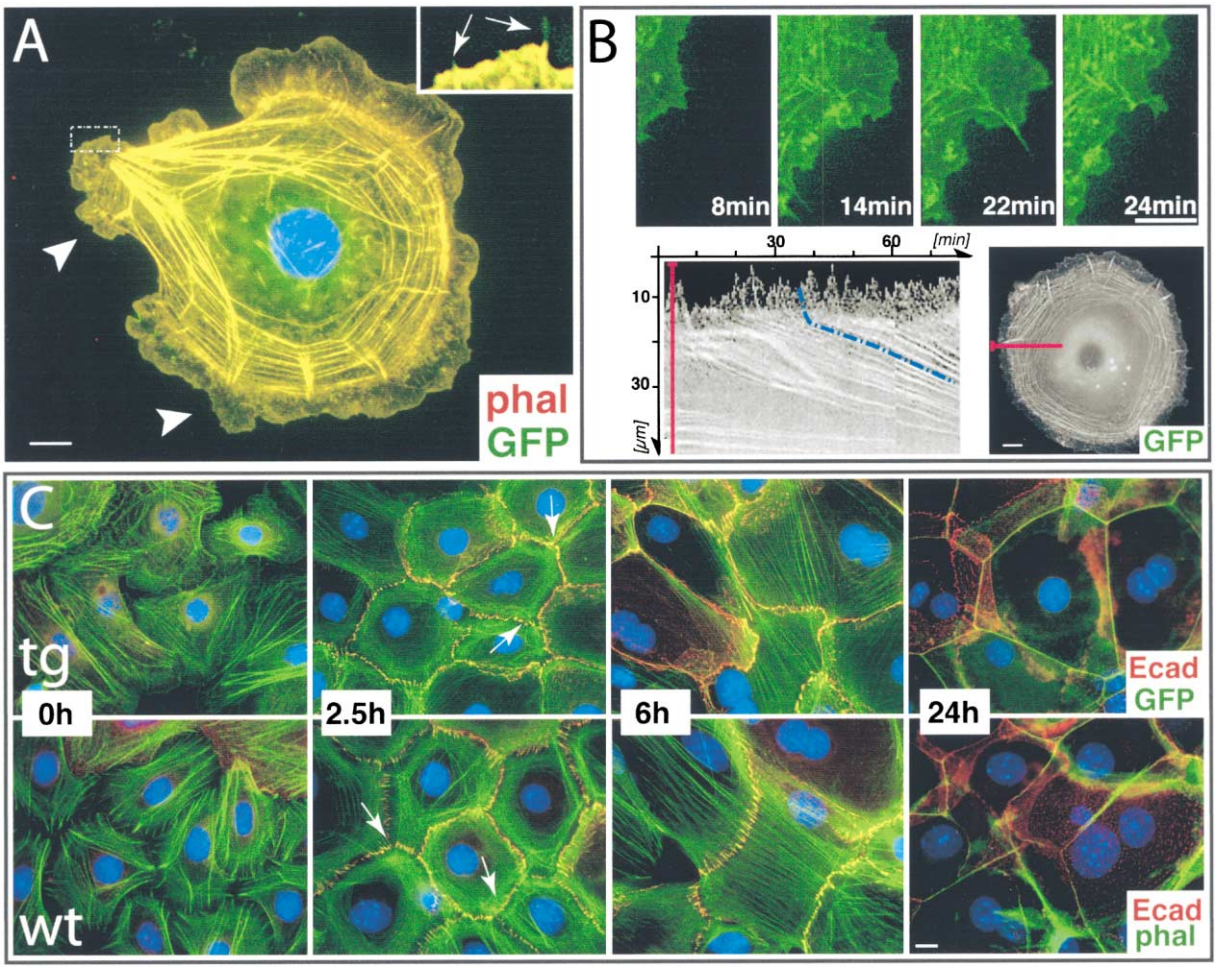

Figure 2. GFP-Actin Dynamics in Solitary Keratinocytes and a Comparison of GFP-Actin and Actin Networks in Keratinocytes Undergoing Adhesion Zipper and Sheet Formation

(A and B) Freshly isolated epidermal keratinocytes were seeded at ~30% confluence in low-calcium medium for 24 hr and then either imaged directly (A) or switched to high-calcium medium for 2 hr (B).

(A) Solitary keratinocytes were processed for fluorescence with GFP and rhodamine-labeled phalloidin. Note that GFP labeling paralleled phalloidin staining, except for a perinuclear GFP-positive haze of nonfilamentous actin, confirmed by anti-β-actin (data not shown). Arrowheads, lamellipodia; arrows, filopodia. Area encased by white dotted box is magnified in inset.

(B) Primary keratinocytes were imaged by video microscopy for 1 hr in low-calcium medium and then for an additional 2 hr in high-calcium medium (see Supplemental Movie S1 at http://www.developmentalcell.com/cgi/content/full/3/3/367/DC1). Upper panels illustrate still frames taken from the movie at times after calcium switch. The images captured of the keratinocyte were subjected to kymograph analysis to monitor the actin fiber movements over time along the line indicated on the cell in the lower frames. A representative actin fiber is highlighted in blue, to illustrate that the velocity of actin (μm/minute) is greatest at the cell periphery and slower within rings.

(C) Keratinocytes were plated at 80% confluence in low-calcium medium for 24 hr, and then there was a shift to high-calcium medium for the times indicated. Cells were fixed and stained with anti-E-cadherin antibodies (red) and either visualized for GFP (transgenic) or FITC-phalloidin (littermate). Note the presence of adhesion zippers (arrows), intermediates in interepidermal membrane sealing that typically form between 1.5 and 4 hr after calcium treatment (Vasioukhin et al., 2000). Bars represent 10 μm.

1995; Vasioukhin et al., 2000). Thus, although a mixture of filopodial and lamellipodial projections appeared to be an essential initial step in bringing membranes together and promoting stable cell contacts, cellular retractions in the presence of these stable adhesion contacts exaggerated these projections.

The formation of a stable contact coincided with the appearance of an associated radial bundle of actin filaments (see Supplemental Movie S2A; Figures 3B and 3C). Additional contacts, each with a bundle of radial actin fibers, soon emerged at sites adjacent to the initial stable contact (Figure 3C). In both temporal and visual appearance, these structures resembled adhesion zippers. Their identity was confirmed by fixing and labeling cells with anti-E-cadherin antibodies and then imaging for GFP (see Figure 2C). Thus, adhesion zippers appeared to be bona fide intermediates in sheet formation in living epidermal cultures, with the initial puncta site being the rate-limiting step of their assembly.

The stability of the extensive network of adhesion zippers was confirmed by extracting cultures with cytoskeletal buffer and labeling with anti-E-cadherin antibodies (Figure 3D). By 1.5–4 hr after the calcium switch, adhesion zippers became prevalent (Figure 3E). The

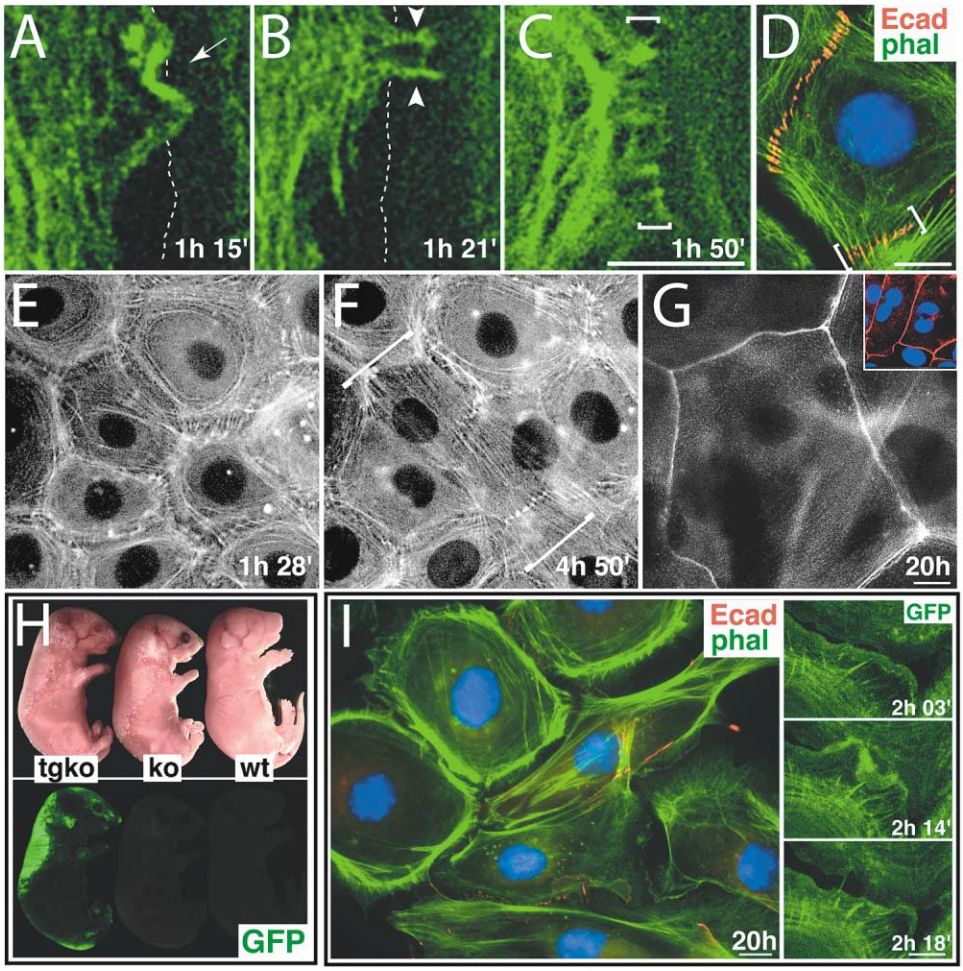

Figure 3. Assembly and Dynamics of an Integrated Cytoskeleton throughout an Epidermal Sheet and Its Reliance on Adherens Junctions

Primary keratinocytes from GFPactin (A–G; see Supplemental Movies S2A and S2B at http://www.developmentalcell.com/cgi/content/full/3/3/367/DC1) and GFP-actin/α-catenin conditional null (H and I; see Supplemental Movie S2C) mice were plated in low-calcium medium at high density (~85% confluency). After 24 hr, cells were imaged by video microscopy, and calcium was elevated at t = 30 min. Recorded times after calcium switch are noted on frames.

(A–C) Still frame, time-lapse images (0.1 μm/pixel) from Supplemental Movie S2A, filmed as keratinocytes formed an adhesion zipper. Dotted white lines denote border of cell at right. Initial successful contact between two cells (arrow) was followed by retraction, which exaggerated the filopodial-like structures (arrowheads). Fully formed adhesion zipper is denoted by brackets.

(D) Keratinocytes after extraction with cytoskeletal buffer and labeled with phalloidin and E-cadherin antibodies. Adhesion zippers (brackets) were prevalent throughout.

(E–F) Still frames from Supplemental Movie S2B, depicting later stages of formation of living epidermal sheets. Note that the actin network spans over multiple cells (brackets in [F]; see also Figure 3 [6h]).

(G) Representative view of culture imaged at 20 hr. Note the honeycomb of cortical actin belts, which, at this stage, correspond to continuous lines of anti-E-cadherin at cell borders (inset).

(H) GFP-actin/α-catenin conditional null mice. Shown are representative littermates from a mating of α-catenin fl/fl, GFP-actin$^{+/+}$ transgenic animals (tg) with α-catenin fl/+, K14Cre$^{+/-}$ mice (Vasioukhin et al., 2001). Mice were imaged by epiluminescence (top) and GFP epifluorescence (bottom) microscopy. Note the presence of a GFP fluorescing animal exhibiting the blistered skin defect of α-catenin conditional knockout mice (tgko).

(I) Keratinocytes derived from GFP-actin/α-catenin conditional null mice. Shown are phalloidin/E-cadherin-stained knockout keratinocytes and still frames of live tgko keratinocytes from Supplemental Movie S2C. Bars denote 10 μm.

double row of puncta (Vasioukhin et al., 2000) appeared to arise as a consequence of both cells tugging on the puncta. As additional puncta formed and intercellular adhesion was strengthened, the putative splitting of puncta seemed to wane.

Through visualizing actin dynamics in living epithelial sheets, we saw that, as a direct consequence of the anchorage of cell-contact-associated radial actin fibers to the dynamic flux of actin rings, the actin network throughout the sheet became continuous, as though the entire sheet shared a single cytoplasm (see Supplemental Movie S2B; Figure 3F; see also Figure 2C [6h]). This elegant actin network did not involve individual actin filaments, but rather gross rearrangements of bundles or cables of actin filaments. The centripetal tension-based movements initially seen within individual cells

were now integrated, yielding inward contractions within the sheet.

As cell-cell contacts increased, radial actin bundles on all sides of the cell tugged on the actin rings, slowing ring flux (see Supplemental Movie S2B). Eventually, the cytoskeleton formed a thick cortical belt of actin visible as a honeycomb network (Figure 3G). The timing of appearance of these cortical belts coincided with continuous lines of anti-E-cadherin staining at cell-cell borders (Figure 3G, inset). These actin dynamics were consistent with the view that actin ring formation and treadmilling is a process that ceases when the barbed ends of actin filaments are firmly attached to a membrane or in areas behind mature cell-cell contacts (Gloushankova et al., 1997).

In contrast to membrane ruffling and lamellipodia formation, the formation of radial actin fibers was dependent upon calcium-induced intercellular contacts. To verify this, we mated our K14-GFP-actin mice with mice conditionally null for α-catenin, the protein required for cytoskeletal coupling to adherens junctions (Vasioukhin et al., 2001, and the references therein). The α-catenin null/GFP-actin mice fluoresced and exhibited blistered skin (Figure 3H). Primary keratinocytes derived from these animals exhibited lamellipodia, filopodia, and the inward flux of concentric rings of actin fibers. They failed to form adhesion zippers, integrated networks of radial actin fibers, or epithelial sheets (see Supplemental Movie S2C; Figure 3I). Overall, their behavior in high calcium resembled that of control keratinocytes in low calcium (compare Supplemental Movie S2C with Supplemental Movie S1).

Adhesion Zippers Organize Actin Fibers into an Integrated Apical Network that Leads to a Top-Down Progression of Membrane Sealing

The morphology of keratinocyte cultures changed as cells made multiple stable intercellular contacts. Solitary keratinocytes were flat, but cells in the developing epithelial sheet organized into a honeycombed network with a thicker cytoplasm. By capturing fluorescent images in horizontal planes, we discovered that, while classical focal contacts and actin stress fibers localized to the basal plane of the monolayer, an elaborate network of radial actin cables and intercellular junctions assembled in the apical zone (Figures 4A and 4B). Staining with anti-vinculin antibodies and imaging for GFP underscored the differences in these networks.

As adhesion zippers became numerous and epithelial sheet formation progressed, the movement of cell borders within the apical plane began to slow, concomitant with the formation of thick cortical belts of actin within the apical zone (see Supplemental Movies S2B and S3A http://www.developmentalcell.com/cgi/content/full/3/3/367/DC1). Actin dynamics persisted in the basal zone, concomitant with classical stress fibers and focal contacts (Figures 4C and 4D; see Supplemental Movie S3A). During the initial stages of polarization, Z stack images indicated that most regions were a monolayer (see Supplemental Movie S3B). Apical and basal images of GFP-labeled keratinocytes surrounded by nontransgenic keratinocytes (mosaic cultures) supported this view. The apical surfaces were part of the honeycomb, and their bases were spread onto the substratum (Figure 4C, inset). As a consequence of this polarization, cells that remained firmly attached to their substratum displayed only a small surface within the honeycomb (examples in Figure 4C), while suprabasal cells that stratified exposed a large honeycomb surface. As stratification increased, the honeycombs became larger and more uniform.

Continued movement of the epidermal monolayer beneath the apical plane led to enhanced overlap of cellular membranes within the midplane (see Supplemental Movie S3A). These overlapping areas contained E-cadherin-positive puncta (Figure 4E). While similar in appearance to puncta in adhesion zippers, these structures organized parallel to, and below, the radial actin cables of more mature junctions (Figure 4E, inset). Imaging verified that these puncta were beneath the honeycomb lattice of continuous E-cadherin-positive staining, suggesting that nascent junctions continued to form beneath this stable apical plane of interconnected epidermal cells (Figure 4F; same cells as in Figure 4E, visualized at a higher plane; the Z stack of these cells is shown in Supplemental Movie S3C). As epidermal cells stratified, they flattened, and E-cadherin labeling became restricted to continuous lines at cell-cell borders.

Ultrastructural Insights into the Process of Epidermal Colony Formation

We next used ultrastructural analyses to explore the process of junction formation in developing epidermal colonies. At early times in the process (0–3 hr), cells made contact through cellular extensions, reflective of the lamellipodial and filopodial protrusions seen at the immunofluorescence level. The first junctions to form were adherens junctions, localized predominantly to sites of cellular overlap (Figures 5A and 5B). This resulted in their positioning above the plane of the substratum, i.e., in the zone where we detected adhesion zippers and radial actin fibers.

The polarization of intercellular junctions became increasingly apparent over time. By 3–6 hr, nascent desmosomes appeared in the apical zone (Figure 5C), reflective of maturing intercellular contacts (Vasioukhin et al., 2000). The prevalent apical membrane interdigitations (Figures 5C and 5C′) were consistent with the numerous adhesion zippers seen in the apical zone of these cultures at this time. Consistent with this polarity, of the nascent desmosomes in representative 6 hr cultures ($n = 32$), approximately 82% resided in the sector encompassing the upper third of the sheet, and none were detected in the lowest sector. By 6–12 hr, adherens junctions were seen in the midsector (Figures 5C′ and 5D). In many cases, the midzone junctions were not perpendicular to the plane of the culture, and the membrane protrusions extended from the underlying cell (example in Figure 5C′). By 12 hr, nascent desmosomes were often detected in this midzone, while the apical zone was now rich with larger desmosomes, containing well-defined inner plaque structures in most of the sealed membrane areas (Figures 5C–5E). Of the desmosomes in representative 12 hr cultures ($n = 91$), $\sim$67% were mature and resided largely in the apical zone, while

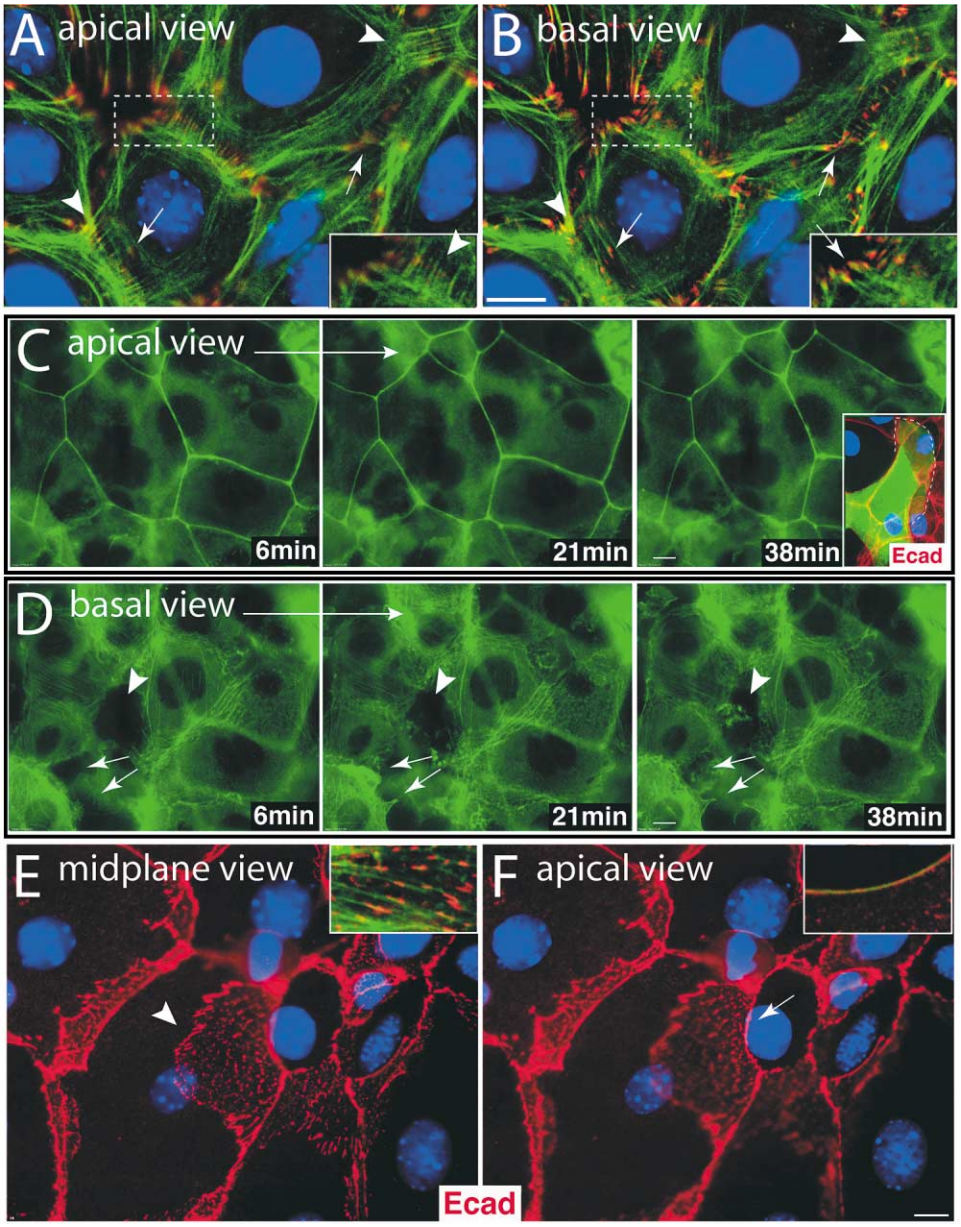

Figure 4. Adherens Junctions Catalyze Polarization of a Tension-Based, Apical Actin Network

Primary keratinocytes were plated for 12–24 hr in low-calcium medium and then switched to high-calcium medium. Video microscopy was used to follow GFP-actin architecture and dynamics within different planes of the epidermal culture (see Supplemental Movie S3A at http://www.developmentalcell.com/cgi/content/full/3/3/367/DC1).

(A and B) Cultures were fixed after 2.5 hr in high calcium and labeled with anti-vinculin and Texas red secondary antibody and FITC phalloidin. The apical (~0.6–0.8 μm) and basal (0 μm) planes of the monolayer are shown. Insets denote magnified views of boxed areas. In the apical plane, adhesion zippers are in focus (arrowheads), and, in the basal plane, focal contacts are in focus (arrows). Both are vinculin positive. Note that, at these early stages, cells are still relatively flat, but the polarized actin cytoskeleton is already visible.

(C and D) After 20 hr in high calcium (t = 0), keratinocytes were subjected to video microscopy (see Supplemetnal Movie S3A). Still frames of the apical and basal planes of cells imaged in movie. Note the paucity of actin dynamics in the apical plane relative to that in the basal plane. Arrowhead in (D) denotes a gap, which becomes invaded by a lamellipodium. Arrows denote actin dynamics involving lamellipodial and filopodial-like extensions. Inset to (C) shows apical view of fluorescent cell wedged among unlabeled cells, making it easy to visualize that the apical plane of the cell is part of the honeycomb network, while the base (encased by the white dotted line) is attached to the substratum and out of the plane of focus. The Z stack of cells imaged in Supplemental Movie S2B shows that, even at early stages of sheet formation, the actin cytoskeleton becomes polarized (see Supplemental Movie S3B).

(E and F) After 10 hr in high-calcium medium, these cells were fixed and stained with anti-E-cadherin (red). Shown are images from the same cell, depicting puncta in the midplane (arrowhead) and mature junctions in the apical plane (arrow). Insets are stained with anti-E-cadherin (red) and FITC phalloidin to illustrate the relation between nascent and mature junctions and their associated radial actin cables. Dapi (blue) was used to stain nuclear DNA. Bars denote 10 μm. Supplemental Movie S3C provides a Z stack of these images.

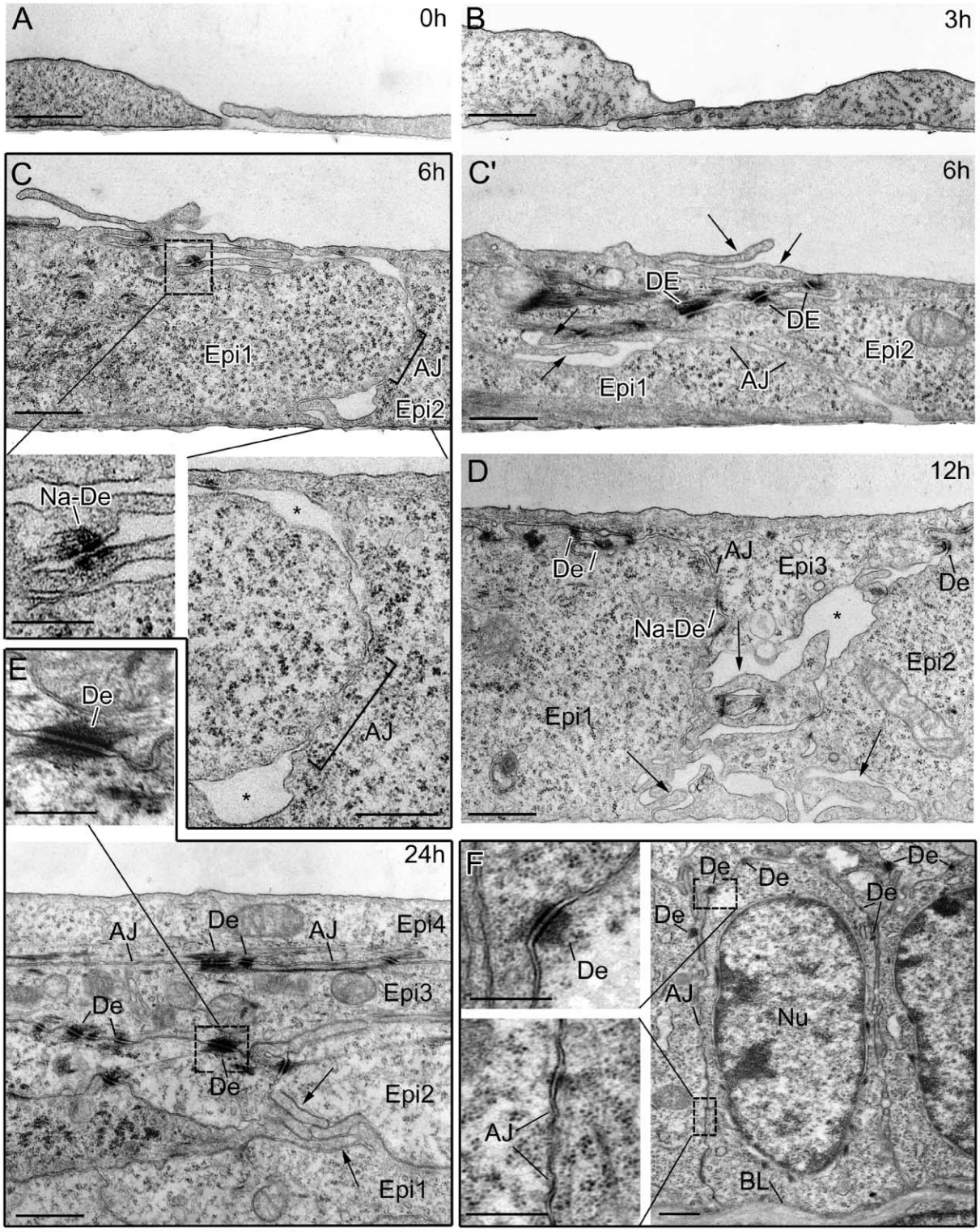

Figure 5. Ultrastructural Analyses of the Polarity of Cell-Cell Adhesion during Epidermal Sheet Formation

(A–E) At 24 hr after plating on ECM-coated permanox slides (Nunc), epidermal keratinocytes were switched from low- to high-calcium medium for the times indicated. Following treatment, cultures were fixed in 2% glutaraldehyde, 1% osmium tetroxide, and 2% aqueous uranyl acetate and embedded in Epon. Cut vertically to the culture plane, ultrathin sections were contrasted with uranyl acetate and lead citrate and examined with a Philips CM 120 microscope. For each time point of each experiment, we made multiple sections of representative areas of the cultures and divided them into apical, midplane, and basal sectors. The total numbers of AJs, Na-Des, and Des in each sector were then counted and expressed as percentages of the total number (n) (see text for values).

(F) Representative cell from basal layer of in vivo epidermis, illustrating lateral surfaces with mostly adherens junctions (magnified at bottom left) and an apical surface with a larger number of desmosomes as well as adherens junctions (magnified at upper left). Stratified layers exhibited more numerous desmosomes (data not shown). De, desmosome; Na-De, nascent desmosome; AJ, adherens junction; Nu, nucleus; BL, basal lamina of extracellular matrix separating dermis and epidermis; Epi 1, 2, etc.; individual epidermal cells; arrows, membrane projections; asterisks, intercellular gaps. Bars represent 10 μm in all main frames and 500 nm in magnified regions.

nascent desmosomes resided in the apical (80%) and midzones (20%). This timing coincided with the development of continuous E-cadherin-positive lines in the apical zone and with the appearance of disorganized E-cadherin-positive complexes in the midzone (see Figure 4). Overall, while the cultures were not completely uniform, they seemed to follow a general sequence of apical to basal junction formation and maturation.

By 24 hr, the centers of some keratinocyte colonies had stratified. The flattened epidermal cells with no apparent substratum contacts often displayed intercellular contacts that were uniformly replete with mature desmosomes alternating with adherens junctions (Figure 5E). Mature desmosomes ($n = 128$) now predominated (99%) and were seen not only in the apical zone (47%), but also in the midzone (46%) and basal zone (7%). Even at this late time, however, membrane dynamics still persisted in the basal zone, where intercellular surfaces had not sealed.

Interestingly, the organization of intercellular junctions within epidermal cultures was similar to that seen in the basal layer of the epidermis in vivo. In epidermis, the lateral surfaces of basal cells exhibited numerous adherens junctions, while the apical surface typically displayed more desmosomes (Figure 5F). Analogously, stratified layers exhibited more numerous desmosomes than basal cells.

Activated Rock Is Essential to Maintain the Apical Plane of Radial Actin Cables and Adhesion Zippers

The bundling of actin fibers during adhesion zipper formation led us to wonder whether this phase of adhesion is controlled by activated Rho, known to accompany calcium-stimulated mouse keratinocyte cultures (Braga et al., 1997; 1999; Calautti et al., 2002). Microarray analyses revealed the presence of RhoA, RhoB, and RhoC mRNAs in our keratinocyte cultures (A. Kobielak, H. Rhee, and E.F., unpublished data), and, using a GST pull-down assay (Noren et al., 2001), we confirmed that GTP-bound Rho is present during adhesion zipper formation (data not shown). Additionally, when primary keratinocytes were transfected with the Rho inhibitor CMV-EGFP-C3 (Sekine et al., 1989), intercellular adhesion and radial actin fibers were markedly perturbed in $\sim$85% of transfected cells (Figure 6A). Such effects were not observed in keratinocytes expressing either a wild-type form of Rho or GFP alone (Figures 6B and 6E). Collectively, these data supported a role for active Rho in the process.

Microarray analyses also revealed a number of possible downstream Rho effectors in keratinocytes, including Rho-activated kinases (Rock) I and II, myosin phosphatase, mDia 1, LimK2, phospholipases D1 and D2, and citron kinase. Of these, Rock is known to be involved in focal contact formation (Katoh et al., 2001; for reviews see Hall, 1998; Ridley, 2001; Geiger and Bershadsky, 2001), a process that resembled the actin dynamics we had observed in adhesion zipper assembly. Indeed, keratinocytes expressing a kinase dead (KD), Rho binding site mutant (Ile to Ala mutation) version of Rock (Rock-KDIA), but not wild-type Rock, exhibited a dramatic reduction in adhesion zipper fibers (Figures 6C and 6D). Puncta and zippers were also impaired as a consequence of dominant-negative Rock expression (Figure 6E).

Rock can indirectly activate myosin II (Amano et al., 2000), which associated in a striated pattern with the central actin network in adhering epidermal cells (Figure 7A). Interestingly, anti-myosin II labeling was reduced over the radial actin cables at adhesion zippers, where actin polymerization is known to occur (Vasioukhin et al., 2000). These sites labeled with antibodies against α-actinin, an actin crosslinking protein not known to be regulated by Rock (Figure 7A).

To pursue the possibility that Rock might exert an indirect effect on adhesion zippers by means of the ability of radial zipper cables to link to the central actomyosin architecture, we employed the Rock inhibitor Y27632. Y27632 specifically binds to the ATP binding site of the catalytic domain of Rock (Narumiya et al., 2000), with an affinity that is $>$20 times higher than that of two other Rho effector kinases, citron kinase and protein kinase PKN (Ishizaki et al., 2000). We also used the less specific drug HA1077 [1-5-(isoquinoline sulfonyl)-homopiperazine HCl], known to inhibit Rock and myosin light chain kinase (Amano et al., 2000, and the references therein). The effects of the two drugs on epidermal keratinocytes were similar, and they were comparable to those of dominant-negative Rock (see Figure 6E). We report here the data for Y27632.

Y27632 markedly perturbed the myosin II pattern in developing epidermal sheets (Figures 7A and 7B). In addition, α-actinin, which is not an integral component of adherens junctions (Vasioukhin et al., 2000), now localized to cell borders, a feature observed irrespective of whether cells made intercellular contact. The effects of Y27632 were similar whether it was added prior to, or after, the formation of adhesion zippers, suggesting that it affected both assembly and maintenance of cytoskeletal architecture at this stage. Concomitant with the reduction in anti-myosin II staining of the apical actin network was a dramatic loss of tension, evident by video microscopy of these cultures (see Supplemental Movie S4 at http://www.developmentalcell.com/cgi/content/full/3/3/367/DC1). Thus, upon Y27632 treatment, cells flattened and no longer displayed the typical tugging and pulling seen in untreated cultures.

As expected from prior studies on stress fiber formation (Maekawa et al., 1999; Amano et al., 1997), Y27632 displayed a striking effect on actin bundling. This was true not only for stress fibers, but also for the radial actin cables associated with adhesion zippers (Figures 7C–7F; see Supplemental Movie S4). Adhesion zippers, so prevalent in normal cultures, were replaced by continuous lines of E-cadherin, anti-VASP, and anti-vinculin staining at cell membranes (7C–7F). While labeling intensities were diminished, particularly with anti-VASP, the impression was a more rapid formation of intercellular contacts. Rock inhibitor also affected the nascent junctions and associated actin cables that normally appear in the midplane of developing epidermal sheets (Figures 7G and 7H). However, as noted previously (Braga et al., 1999, 2000; Sahai and Marshall, 2002), the drug had little effect on fully developed epithelial sheets. Overall, Rock inhibitors appeared to perturb cytoskeletal dynamics and intercellular junctions in early, but not late, stages of epithelial sheet formation.

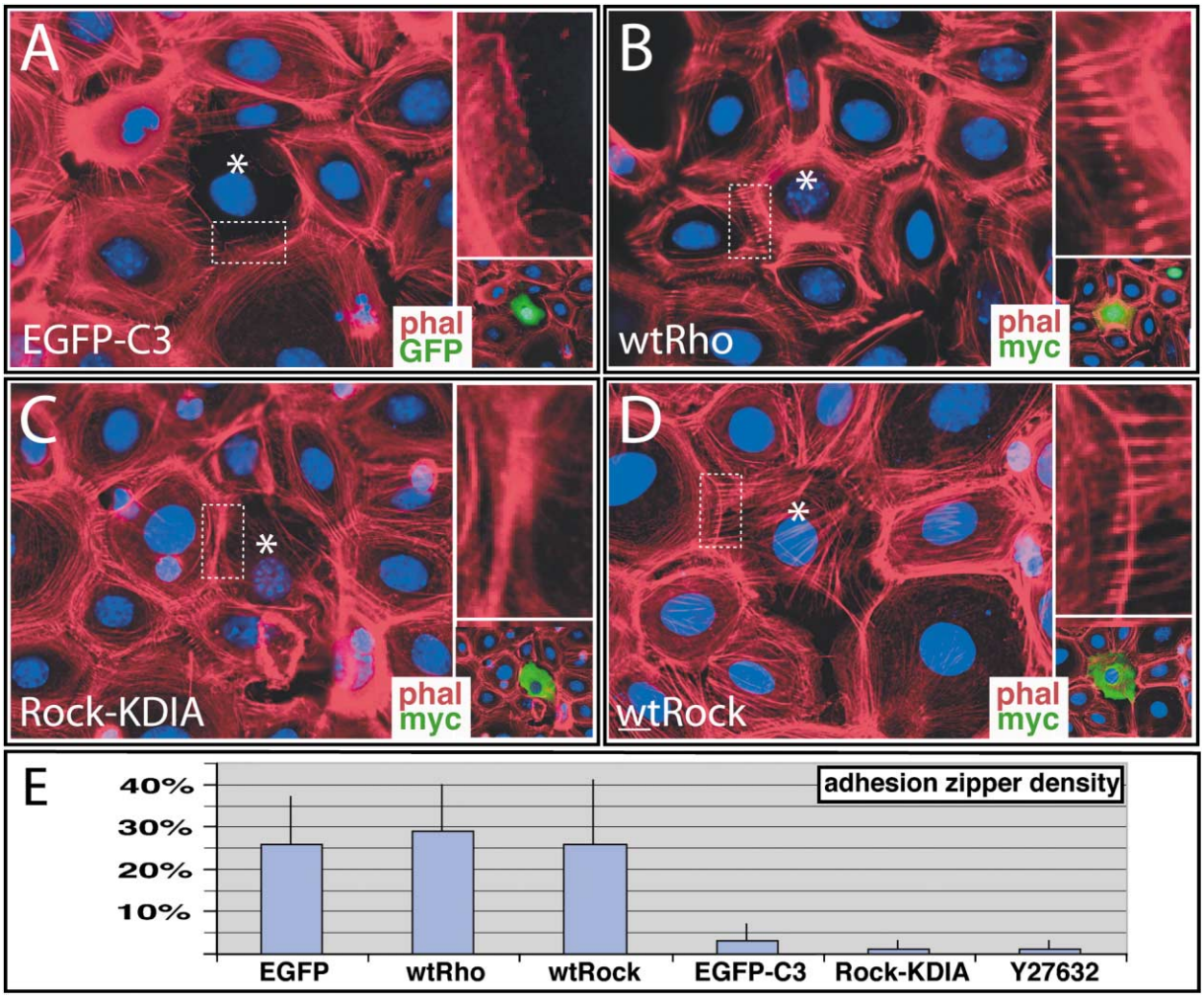

Figure 6. Expression of Rho and Rock Inhibitors in Individually Transfected Keratinocytes Results in Defects in Adhesion Zippers

Primary epidermal keratinocytes were transfected with cytomegalovirus (CMV) expression vectors encoding the Rho inhibitor GFP-tagged C3, or c-*myc* epitope-tagged versions of wild-type RhoA, dominant-negative Rock (Rock-KDIA), or wild-type Rock. Forty-eight hours after transfection, cultures were fixed and processed for fluorescence microscopy with Dapi (blue) and phalloidin (red). Costaining in green (insets) marks the transfected cells (asterisks) shown in the main frames. Insets in upper right show magnified views of boxed areas. Bar represents 10 μm.

(E) Quantitation. The cell-cell borders of transfected or chemically inhibited cultures were analyzed for the percentage of intercellular contact that is occupied by adhesion zippers in two-dimensional space (adhesion zipper density). Note that ~90% of the cells treated with Rock or Rho inhibitors displayed perturbed stress fibers and that these were selected for analyses. Relatively large error bars reflect heterogeneity in adhesion zipper densities throughout the cultures.

Discussion

By monitoring actin dynamics in primary epidermal cells from physiologically normal, GFP-actin transgenic mice, we discovered that keratinocytes undergo extensive remodeling of their actin cytoskeleton during epithelial sheet formation and stratification. This process begins at the level of individual cells, but progresses to orchestrated movements of the actin network that extends across the entire epithelial sheet. The organization of actin filaments associated with the early steps in intercellular adhesion is polarized, and begins at the apical surface of the epidermal monolayer. The polarized actin framework that assembles at adhesion zippers and generates an integrated cellular network of actin cables may be important in producing and maintaining the epidermal barrier and in facilitating the process of stratification.

Actin Dynamics and the Role of Rock in the Early Steps of Epithelial Sheet Assembly

The tension-based network of actin cables and adhesion zippers that formed in the apical plane of the developing epidermal sheet was remarkably similar to, and is likely to be interconnected with, the extensive actin stress fibers and focal contacts that form at the base of the monolayer. For this reason, our studies naturally gravitated toward Rho, Rock, and myosin activation as a candidate pathway for governing at least some of the features of this polarized architecture.

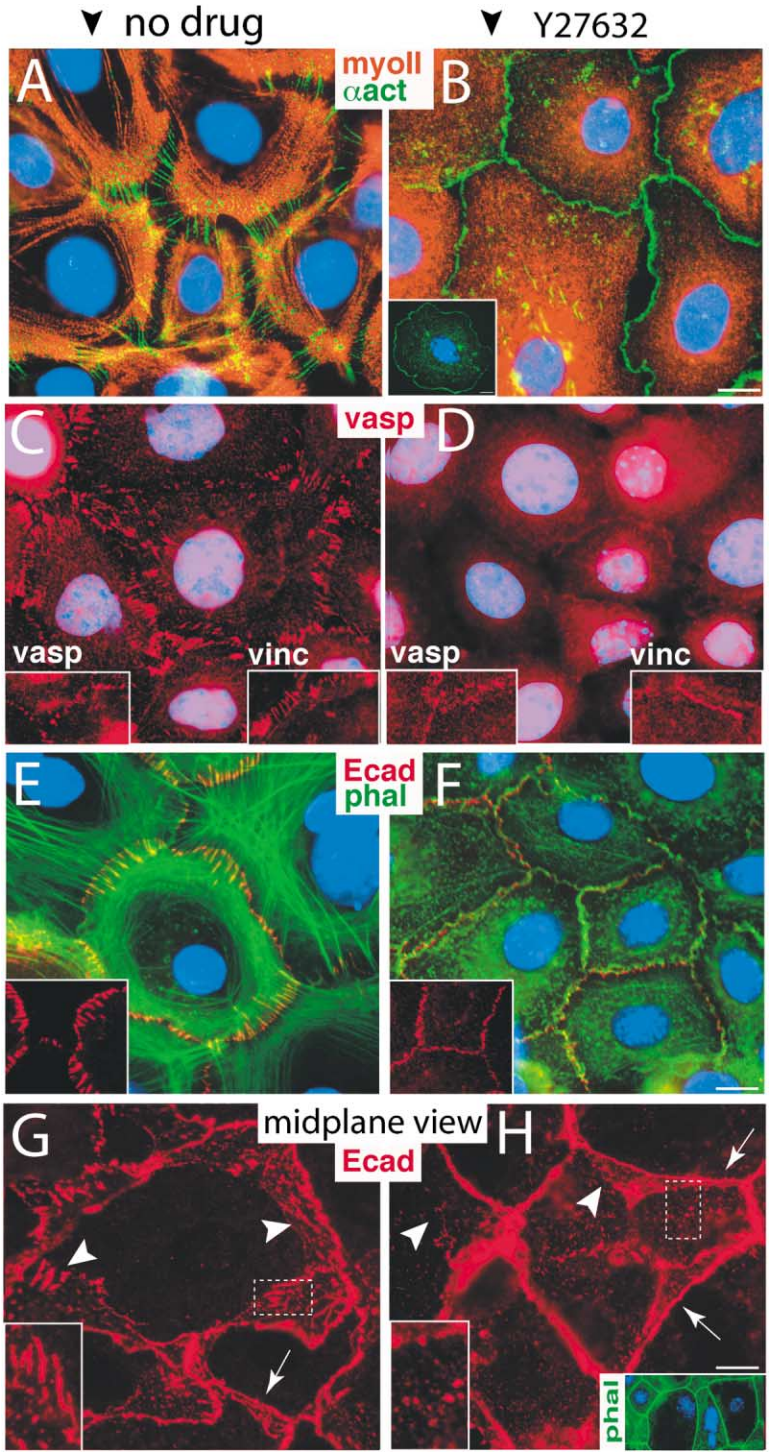

Figure 7. Rock Inhibition by Y27632 Reveals Dramatic Effects on Polarized Actin Cable Dynamics and Nascent Intercellular Junctions in Developing Epidermal Sheets

Primary epidermal keratinocytes were cultured 24 hr and then pretreated with 15 μM Y27632 (Yoshitoni Pharmaceutical Industry, Fukuoka-ken, Japan) for 30 min prior to the addition of high-calcium medium. Whenever drug was added (right panels), it was replaced three times at intervals of 60 min. Cells were then processed for immunofluorescence microscopy.

(A and B) Anti-myosin II, anti-αactinin. Inset to (B) illustrates that, even in solitary keratinocytes, drug treatment results in cell border localization of α-actinin.

(C and D) Anti-Vasp. Insets show magnified views with enhanced staining to visualize labeling at cell-cell borders. Note the marked reduction in VASP at junctions after Rock inhibition.

(E and F) Anti-E-cadherin, FITC phalloidin. Insets show anti-E-cadherin alone to illustrate punctate labeling in untreated, and more-linear labeling in treated, cultures. Note that, in (F) and in its inset, the E-cadherin lines, while continuous, are not straight.

(G and H) Cells were cultured 10 hr in high-calcium medium prior to the addition of control buffer (G) or drug (H) for 30 min, and then they were fixed and labeled with anti-E-cadherin. Nascent junctions (puncta) in the midplane of untreated cultures are disorganized and fewer upon drug treatment. Continuous lines of E-cadherin give the impression that adhesion is accelerated by Y27632. Inset to (H) shows culture exposed to high-calcium medium for 24 hr prior to the addition of Y27632. Actin (shown) and anti-E-cadherin (data not shown) stainings were unperturbed. Bars denote 10 μm. Following Y27632 treatment, cells were examined by video microscopy (see Supplemental Movie S4 at http://www.developmentalcell.com/cgi/content/full/3/3/367/DC1).

Our findings provide insights into earlier studies of Braga et al. (1997; 1999; 2000) and Calautti et al. (2002), who first reported the deleterious effects on keratinocytes treated with Rho, but not Rock, inhibitors. These researchers concluded that Rho's and Rock's effects on intercellular adhesion must not be dependent upon their ability to bundle actin fibers and generate tension (Braga, et al., 2000), and their interpretation was substantiated by the finding that activated RhoA promotes cell-cell adhesion in a Fyn tyrosine kinase-dependent, actin-independent manner (Calautti et al., 2002). While our results fit within this framework, they suggest an actin-dependent role for RhoA and Rock in higher-ordered architecture, namely in generating the tension-based, polarized structure of a developing epidermal sheet.

Our results suggest that Rock inhibition may directly affect the central myosin II-decorated actin cables in

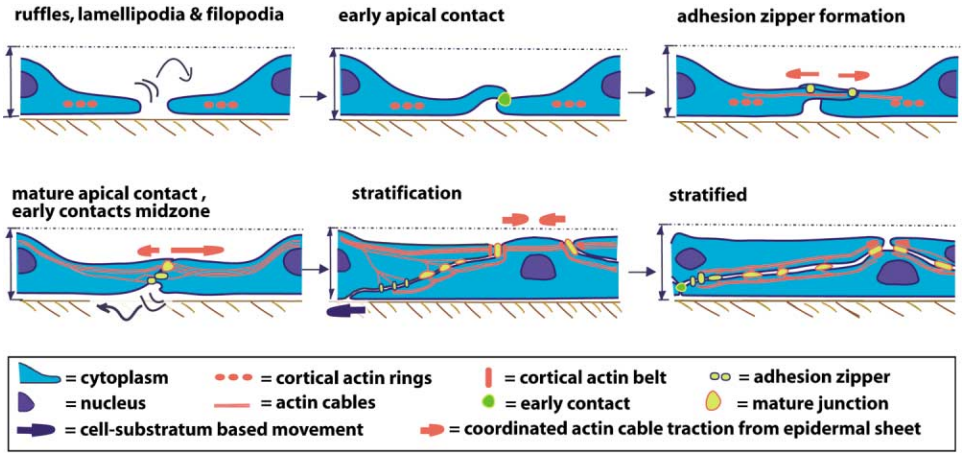

Figure 8. Model for Epidermal Stratification

Model depicts possible mechanism for epidermal stratification. This mechanism is based upon a top-down assembly of stable intercellular junctions and upon an initial myosin-based centripetal movement of actin fibers within solitary keratinocytes. As junctions form, a polarized apical architecture of actin cables and adherens junctions (adhesion zippers) assembles, which, over time, results in a network of actin cables that extends throughout the epidermal sheet. Through integrated tension-based movements within the sheet, cells in the center pull those at the periphery to begin the process of stratification. Beneath the apical plane, actin dynamics continue, enabling cells to move outward, generating nascent intercellular junctions beneath the apical plane, and eventually displacing neighboring cells to generate a stratified tissue. The polarized actin architecture across the sheet is sensitive to Rock inhibitors, which impair this process.

epidermal keratinocytes. Through their associated radial actin fibers, adhesion zippers anchor to, and polarize, this network. When the integrated tension generated by this network is released, adhesion zippers relax, the actin cytoskeleton loses its apical polarity, keratinocytes flatten, and membrane contact is accelerated. The outcome appears to be a gain in the kinetics of adhesion, as recently indicated from studies on other epithelial cell types (Wojciak-Stothard et al., 2001; Sahai and Marshall, 2002). The downside, however, may be a disorganization of nascent junctions and impairment of the cellular movements necessary to form and/or maintain the precise architecture of the developing tissue. This may be particularly deleterious under the conditions such as those monitored here, where overall cellular architecture has not yet been reinforced by an extensive framework of desmosomes and intermediate filaments. An interesting parallel may be dorsal closure of the embryonic fly epidermis, a process that resembles wound healing in mammalian epidermis. Rho GTPases have long been implicated in dorsal closure, and, recently, both positive and negative roles for myosin II regulation have been uncovered (Mizuno et al., 2002; Bloor and Kiehart, 2002).

Cell-type-Specific Parallels and Differences in Polarized Actin Cytoskeletons

Our discovery of a polarized, Rock-regulated, apical actin cytoskeleton reminded us of observations made by Nusrat et al. (1995), who first identified Rho-dependent apical polarized actin architecture in intestinal epithelial cell lines. Interestingly, this architecture in simple epithelial cells has been linked to tight junctions and their ability to function properly as molecular gates (Nusrat et al., 1995; Walsh et al., 2001; Jou et al., 1998), whereas the Rock-dependent radial actin cables in our primary epidermal cells were associated with E-cadherin-rich adhesion zippers. In part, this difference seems likely to result from the fact that, in a stratifying tissue such as epidermis, tight junctions form late relative to adherens junctions (Furuse et al., 2002; Bazzoni and Dejana, 2002). A Rho/Rock-dependent, polarized actin cytoskeleton that associates with adherens junctions could easily be utilized subsequently by other types of junctions, including tight junctions. A general role for Rock in orchestrating the actin dynamics and cellular junctions necessary to establish a functional three-dimensional epithelium, whether stratified or simple, is further supported by the recent studies of Wojciak-Stothard et al. (2001), who reported that permeability and barrier function are altered when Rock is impaired in endothelial cells.

Possible Functions of an Integrated, Polarized Actin Cytoskeleton in Epidermal Tissue

One advantage to having a polarized apical actin cytoskeleton is that intercellular adhesion can seal membranes and create a barrier at their apical surface while permitting continued actin dynamics and cellular movements beneath this plane. By integrating the network of radial actin cables and intercellular contacts across the apical plane of the developing epidermal sheet, tension-based movements of single cells progress into coordinated and more robust actin-myosin-based contractions within the tissue. Such activity enables the apical surfaces of cells to move relative to their base, a process that substantially increases intercellular contacts between neighboring cells at the expense of cell-substratum contacts. As the developing sheet exerts apical tension on an internal cell, the underlying adherent cells move in from the base, eventually displacing their neighbor from its substratum.

Figure 8 illustrates a model for stratification that is based upon this concept. For simplicity, we have not taken into account stratification factors proposed by others, including differentiation-associated changes in

the expression of intercellular junction genes (reviewed by Kowalczyk et al., 1999; Runswick et al., 2001) and the downregulation in β1 integrin expression, necessary for cell-substratum detachment (Hodivala and Watt, 1994). That said, for any cell where the apical contractile tension of radial actin fibers is weak or absent, the tension across the apical zone of the sheet results in adjacent cells pulling at the surface of their neighbor as a blanket, leading to flattening and stratification of the central cell. Additionally, the model advocates enhanced stratification when cell-substratum adhesion is weakened.

Polarized top-down progression of intercellular junction maturation and tension-based epidermal sheet movements could serve an important function in a self-renewing, stratified tissue like the epidermis, where cells continually exit the basal layer, terminally differentiate, and move outward, creating a constant flux of basal vacancies that must be filled by basal cells moving inward. This mechanism could be especially important in wound healing, where such coordinated movements can rapidly increase both the surface area and the contractile potential of the surrounding epidermis while preserving its ability to function as a barrier.

In closing, how cells polarize their cytoskeletons is of fundamental importance not only to the mammalian epidermis, but also to the development of most higher eukaryotic organisms and their associated tissues. In this regard, it seems relevant that RhoA and Rock have been genetically linked to the establishment of planar polarity in *Drosophila*. This process was first shown to be important for the polarized positioning of a spike, or trichome, on the apical surface of each epidermal cell within the fly's monolayer (Strutt, 2001). A possible thread between planar polarity in fly epidermal cells and mammalian epidermal tissue assembly is their polarized networks of actin cables. What might distinguish these processes is the location within the cell where Rho and its effectors become activated (Winter et al., 2001). An obvious challenge is to elucidate the site and molecular mechanism involved in localizing Rho and its downstream effectors in setting up the polarized plane of actin cables and adhesion zippers in the developing epidermal sheet. Another key avenue for future explorations will be to ascertain the extent to which the polarization of adherens junctions and actin-myosin networks are important in the natural processes of epidermal homeostasis, development, or wound healing.

Experimental Procedures

Preparation of Primary Keratinocytes

Transgenic animals were identified with a GFP fluorescence stereomicroscope, M7 (Leica, Germany). Separation of newborn mouse skin epidermis by dispase, isolation of primary keratinocytes, and culture conditions were as described (Vasioukhin et al., 2000). Twenty-four hours after seeding on glass coverslips coated with collagen I (Collaborative Research, Bedford, MA), AJ formation was induced by increasing the $CaCl_2$ concentration from 0.05 mM to 1.2 mM.

Immunofluorescence

Frozen skin or keratinocytes were fixed in 4% formaldehyde in PBS for 10 min and then subjected to double indirect immunostaining (Vasioukhin et al., 2000). A confocal microscope, LSM 410, was used for analysis on skin, and an Axiovert 100TV was used for cultures (Carl Zeiss, Thornwood, NY). Primary antibodies used were against the following: E-cadherin (ECCD2; Masatoshi Takaishi, Kobe, Japan), vinculin, α-actinin and phalloidin-TRITC/FITC (Sigma, St. Louis, MO), myosin II (BTI, Stoughton, MA), anti-VASP (M4; Alexis, San Diego, CA), anti-laminin 1, anti-myc antibody Clone E9 (Zymed, San Francisco, CA), and DAPI (Sigma). Dilutions were performed according to the manufacturer's recommendations. Fluorescence-conjugated secondary antibodies were from Jackson Immunoresearch Laboratories (West Grove, PA). For cytoskeletal extractions, we incubated cells in the presence of 0.2% Triton X-100, 10 mM HEPES (pH 6.1), 138 mM KCl, 3 mM $MgCl_2$, 2 mM EGTA, and 0.32 M sucrose.

Determination of Transgene and F-Actin Levels in Keratinocytes

Keratinocytes (4×10^6 cells/ml) were lysed in 1 ml of buffer containing 0.6 μM phalloidin, which binds to and stabilizes F-actin, and 10 μM Dnase I, which binds and sequesters monomeric actin (Cano et al., 1992). Equal amounts of total protein were subjected to centrifugation for 30 min at 100,000 × g to pellet actin filaments that contain >50 monomers. Pellet and supernatant fractions were then resuspended in gel sample buffer and subjected to SDS-PAGE, immunoblot analyses, and densitometry. Beta-actin was detected with AC15 antibody (Sigma) and GFP-actin with a GFP monoclonal antibody (University of Chicago). Clone C4 antibody (ICN, Costa Mesa, CA), recognizing both β-actin and GFP-actin, was used to determine transgene levels.

Video Microscopy and Image Analyses

Cells were placed in a closed heat-controlled chamber (FCS2; Bioptechs, Butler, PA) on a Zeiss axiovert 100TV inverted microscope equipped with an automated ludle filter wheel. Video microscopy was performed with a 63× plan apochromatic objective numerical aperture 1.4 equipped with a temperature-controlled heating device (Bioptechs). GFP was excited with a Tungsten 100 W lamp through a GFP excitation filter, and data were acquired with a Micromax CCD camera (Princeton Instruments, Princeton, NJ) at a resolution of 0.1 μm/pixel. Time-lapse images were acquired with Slidebook Software (Intelligent Imaging Innovation, Denver, CO). The movies were edited in Adobe Aftereffects (San Jose, CA). For kymograph analyses, we imported images into MetaMorph software (Universal Imaging, West Chester, PA).

Acknowledgments

A special thank you goes to Jie Fan for generating the transgenic mice used in these studies, Dr. Amalia Pasolli for her assistance in compiling and quantitating EM data, and to Dr. Agnes Kobielak and Horace Rhee for sharing and quantitating their microarray data. We also thank the following people for their generous gifts: Dr. Alan Hall (MRC, University College London, England; dominant-negative and dominant-positive forms of Rho), Dr. Masatoshi Takeichi (RIKEN Institute, Kobe, Japan; anti-E-cadherin antibodies), Dr. Suhu Narumiya (Kyoto University, Kyoto, Japan; dominant-negative and wild-type Rock and EGFP C3 vectors), Keith Burridge (University of North Carolina, Chapel Hill, NC; protocols for detecting activated Rho and other small GTPases), Drs. Vic Small and Irina Kaverina (Salzburg, Austria; protocols for video microscopy). A.V. will receive his PhD from the Committee on Cancer Biology at The University of Chicago. E.F. is an investigator of the Howard Hughes Medical Institute. This work was supported by a grant from the National Institutes of Health.

Received: June 12, 2002
Revised: July 30, 2002

References

Adams, C.L., Nelson, W.J., and Smith, S.J. (1996). Quantitative analysis of cadherin-catenin-actin reorganization during development of cell-cell adhesion. J. Cell Biol. *135*, 1899–1911.

Adams, C.L., Chen, Y.T., Smith, S.J., and Nelson, W.J. (1998). Mechanisms of epithelial cell-cell adhesion and cell compaction revealed

by high-resolution tracking of E-cadherin-green fluorescent protein. J. Cell Biol. *142*, 1105–1119.

Amano, M., Chihara, K., Kimura, K., Fukata, Y., Nakamura, N., Matsuura, Y., and Kaibuchi, K. (1997). Formation of actin stress fibers and focal adhesions enhanced by Rho-kinase. Science *275*, 1308–1311.

Amano, M., Fukata, Y., and Kaibuchi, K. (2000). Regulation and functions of Rho-associated kinase. Exp. Cell Res. *261*, 44–51.

Angres, B., Barth, A., and Nelson, W.J. (1996). Mechanism for transition from initial to stable cell-cell adhesion: kinetic analysis of E-cadherin-mediated adhesion using a quantitative adhesion assay. J. Cell Biol. *134*, 549–557.

Bazzoni, G., and Dejana, E. (2002). Keratinocyte junctions and the epidermal barrier: how to make a skin-tight dress. J. Cell Biol. *156*, 947–949.

Bloor, J.W., and Kiehart, D.P. (2002). Drosophila RhoA regulates the cytoskeleton and cell-cell adhesion in the developing epidermis. Development *129*, 3173–3183.

Braga, V.M., Machesky, L.M., Hall, A., and Hotchin, N.A. (1997). The small GTPases Rho and Rac are required for the establishment of cadherin-dependent cell-cell contacts. J. Cell Biol. *137*, 1421–1431.

Braga, V.M., Del Maschio, A., Machesky, L., and Dejana, E. (1999). Regulation of cadherin function by Rho and Rac: modulation by junction maturation and cellular context. Mol. Biol. Cell *10*, 9–22.

Braga, V.M., Betson, M., Li, X., and Lamarche-Vane, N. (2000). Activation of the small GTPase Rac is sufficient to disrupt cadherin-dependent cell-cell adhesion in normal human keratinocytes. Mol. Biol. Cell *11*, 3703–3721.

Calautti, E., Grossi, M., Mammucari, C., Aoyama, Y., Pirro, M., Ono, Y., Li, J., and Dotto, G.P. (2002). Fyn tyrosine kinase is a downstream mediator of Rho/PRK2 function in keratinocyte cell-cell adhesion. J. Cell Biol. *156*, 137–148.

Cano, M.L., Cassimeris, L., Joyce, M., and Zigmond, S.H. (1992). Characterization of tetramethylrhodaminyl-phalloidin binding to cellular F-actin. Cell Motil. Cytoskeleton *21*, 147–158.

Carlier, M.F. (1998). Control of actin dynamics. Curr. Opin. Cell Biol. *10*, 45–51.

Doyle, T., and Botstein, D. (1996). Movement of yeast cortical actin cytoskeleton visualized in vivo. Proc. Natl. Acad. Sci. USA *93*, 3886–3891.

Furuse, M., Hata, M., Furuse, K., Yoshida, Y., Haratake, A., Sugitani, Y., Noda, T., Kubo, A., and Tsukita, S. (2002). Claudin-based tight junctions are crucial for the mammalian epidermal barrier: a lesson from claudin-1-deficient mice. J. Cell Biol. *156*, 1099–1111.

Geiger, B., and Bershadsky, A. (2001). Assembly and mechanosensory function of focal contacts. Curr. Opin. Cell Biol. *13*, 584–592.

Gloushankova, N.A., Alieva, N.A., Krendel, M.F., Bonder, E.M., Feder, H.H., Vasiliev, J.M., and Gelfand, I.M. (1997). Cell-cell contact changes the dynamics of lamellar activity in nontransformed epitheliocytes but not in their ras-transformed descendants. Proc. Natl. Acad. Sci. USA *94*, 879–883.

Hall, A. (1998). Rho GTPases and the actin cytoskeleton. Science *279*, 509–514.

Hirano, S., Nose, A., Hatta, K., Kawakami, A., and Takeichi, M. (1987). Calcium-dependent cell-cell adhesion molecules (cadherins): subclass specificities and possible involvement of actin bundles. J. Cell Biol. *105*, 2501–2510.

Hodivala, K.J., and Watt, F.M. (1994). Evidence that cadherins play a role in the downregulation of integrin expression that occurs during keratinocyte terminal differentiation. J. Cell Biol. *124*, 589–600.

Ishizaki, T., Uehata, M., Tamechika, I., Keel, J., Nonomura, K., Maekawa, M., and Narumiya, S. (2000). Pharmacological properties of Y-27632, a specific inhibitor of rho-associated kinases. Mol. Pharmacol. *57*, 976–983.

Jacinto, A., Woolner, S., and Martin, P. (2002). Dynamic analysis of dorsal closure in *Drosophila*: from genetics to cell biology. Dev. Cell *3*, 9–19.

Jamora, C., and Fuchs, E. (2002). Intercellular adhesion, signalling and the cytoskeleton. Nat. Cell Biol. *4*, 101–108.

Jou, T.S., and Nelson, W.J. (1998). Effects of regulated expression of mutant RhoA and Rac1 small GTPases on the development of epithelial (MDCK) cell polarity. J. Cell Biol. *142*, 85–100.

Jou, T.S., Schneeberger, E.E., and Nelson, W.J. (1998). Structural and functional regulation of tight junctions by RhoA and Rac1 small GTPases. J. Cell Biol. *142*, 101–115.

Katoh, K., Kano, Y., Amano, M., Onishi, H., Kaibuchi, K., and Fujiwara, K. (2001). Rho-kinase-mediated contraction of isolated stress fibers. J. Cell Biol. *153*, 569–584.

Kowalczyk, A.P., Bornslaeger, E.A., Norvell, S.M., Palka, H.L., and Green, K.J. (1999). Desmosomes: intercellular adhesive junctions specialized for attachment of intermediate filaments. Int. Rev. Cytol. *185*, 237–302.

Maekawa, M., Ishizaki, T., Boku, S., Watanabe, N., Fujita, A., Iwamatsu, A., Obinata, T., Ohashi, K., Mizuno, K., and Narumiya, S. (1999). Signaling from Rho to the actin cytoskeleton through protein kinases Rock and LIM-kinase. Science *285*, 895–898.

Mizuno, T., Tsutsui, K., and Nishida, Y. (2002). Drosophila myosin phosphatase and its role in dorsal closure. Development *129*, 1215–1223.

Narumiya, S., Ishizaki, T., and Uehata, M. (2000). Use and properties of Rock-specific inhibitor Y-27632. Methods Enzymol. *325*, 273–284.

Nakagawa, M., Fukata, M., Yamaga, M., Itoh, N., and Kaibuchi, K. (2001). Recruitment and activation of Rac1 by the formation of E-cadherin-mediated cell-cell adhesion sites. J. Cell Sci. *114*, 1829–1838.

Noren, N.K., Niessen, C.M., Gumbiner, B.M., and Burridge, K. (2001). Cadherin engagement regulates Rho family GTPases. J. Biol. Chem. *276*, 33305–33308.

Nusrat, A., Giry, M., Turner, J.R., Colgan, S.P., Parkos, C.A., Carnes, D., Lemichez, E., Boquet, P., and Madara, J.L. (1995). Rho protein regulates tight junctions and perijunctional actin organization in polarized epithelia. Proc. Natl. Acad. Sci. USA *92*, 10629–10633.

Reinhard, M., Halbrugge, M., Scheer, U., Wiegand, C., Jockusch, B.M., and Walter, U. (1992). The 46/50 kDa phosphoprotein VASP purified from human platelets is a novel protein associated with actin filaments and focal contacts. EMBO J. *11*, 2063–2070.

Ridley, A.J., and Hall, A. (1992). The small GTP-binding protein rho regulates the assembly of focal adhesions and actin stress fibers in response to growth factors. Cell *70*, 389–399.

Ridley, A.J. (2001). Rho proteins: linking signaling with membrane trafficking. Traffic *2*, 303–310.

Runswick, S.K., O'Hare, M.J., Jones, L., Streuli, C.H., and Garrod, D.R. (2001). Desmosomal adhesion regulates epithelial morphogenesis and cell positioning. Nat. Cell Biol. *3*, 823–830.

Sahai, E., and Marshall, C.J. (2002). Rock and Dia have opposing effects on adherens junctions downstream of Rho. Nat. Cell Biol. *4*, 408–415.

Sekine, A., Fujiwara, M., and Narumiya, S. (1989). Asparagine residue in the rho gene product is the modification site for botulinum ADP-ribosyltransferase. J. Biol. Chem. *264*, 8602–8605.

Strutt, D. (2001). Planar polarity: getting ready to Rock. Curr. Biol. *11*, R506–R509.

Takaishi, K., Sasaki, T., Kotani, H., Nishioka, H., and Takai, Y. (1997). Regulation of cell-cell adhesion by rac and rho small G proteins in MDCK cells. J. Cell Biol. *139*, 1047–1059.

Theriot, J.A. (1997). Accelerating on a treadmill: ADF/cofilin promotes rapid actin filament turnover in the dynamic cytoskeleton. J. Cell Biol. *136*, 1165–1168.

Vasioukhin, V., Bauer, C., Yin, M., and Fuchs, E. (2000). Directed actin polymerization is the driving force for epithelial cell-cell adhesion. Cell *100*, 209–219.

Vasioukhin, V., Bauer, C., Degenstein, L., Wise, B., and Fuchs, E. (2001). Hyperproliferation and defects in epithelial polarity upon conditional ablation of alpha-catenin in skin. Cell *104*, 605–617.

Walsh, S.V., Hopkins, A.M., Chen, J., Narumiya, S., Parkos, C.A., and Nusrat, A. (2001). Rho kinase regulates tight junction function and is necessary for tight junction assembly in polarized intestinal epithelia. Gastroenterology. *121*, 566–579.

Winter, C.G., Wang, B., Ballew, A., Royou, A., Karess, R., Axelrod, J.D., and Luo, L. (2001). Drosophila Rho-associated kinase (Drok) links Frizzled-mediated planar cell polarity signaling to the actin cytoskeleton. Cell *105*, 81–91.

Wojciak-Stothard, B., Potempa, S., Eichholtz, T., and Ridley, A.J. (2001). Rho and Rac but not Cdc42 regulate endothelial cell permeability. J. Cell Sci. *114*, 1343–1355.

Yeaman, C., Grindstaff, K.K., and Nelson, W.J. (1999). New perspectives on mechanisms involved in generating epithelial cell polarity. Physiol. Rev. *79*, 73–98.

Yonemura, S., Itoh, M., Nagafuchi, A., and Tsukita, S. (1995). Cell-to-cell adherens junction formation and actin filament organization: similarities and differences between non-polarized fibroblasts and polarized epithelial cells. J. Cell Sci. *108*, 127–142.